2011 IEEE/RSJ International Conference on
Intelligent Robots and Systems
September 25-30, 2011. San Francisco, CA, USA

Denoising of Range Images using a Trilateral Filter and Belief Propagation

Shuji Oishi, Ryo Kurazume, Yumi Iwashita, and Tsutomu Hasegawa

Abstract— **Two denoising techniques using reflectivity for noisy range images are proposed: range image smoothing by trilateral filter and range image inpainting by belief propagation. The trilateral filter makes use of reflectivity as well as spatial and intensity information so that geometric features, such as jump and roof edges, are preserved while smoothing. The range image inpainting technique based on belief propagation recovers a deteriorated range image using not only the adjacent range values but also the continuity of the reflectance image. We conduct simulations and experiments using synthesized images and actual range images taken by a laser scanner and verify that the proposed techniques suppress noise while preserving jump and roof edges and repair deteriorated range images.**

I. INTRODUCTION

In recent years, high-precision three-dimensional (3D) laser scanners, such as RIEGL VZ-400 (RIEGL GmbH), Leica Scan Station 2 (Leica Geosystems AG), and TOPCON GLS-1500 (TOPCON), have been widely used for landscape surveying or digital 3D modeling. In addition, a low-cost, high-resolution laser measurement systems using two-dimensional laser scanners (SICK LMS151 (SICK AG) and HOKUYO TOP-URG (HOKUYO)) and a rotary table have been proposed for 3D environmental map building for mobile robot navigation [1]. These LIDAR (light detection and ranging) sensors acquire high resolution and precise range images. However, range images often suffer from noise due to the reflectance property of objects' surfaces or electrical and mechanical disturbances. For example, one sigma accuracy of RIEGL VZ-400 is 3mm per 100 meters, thus a flat surface is measured as a slightly uneven plate. Metal surface with strong specular reflection or black color cannot be measured by standard laser scanners. Therefore, denoising techniques for range images taken by laser scanners still remains as a critical problem.

In the present paper, we propose two denoising techniques which focus on the reflectivity [2]. When we measure range data by laser scanners, the reflectivity, which indicates the strength of the reflected laser can be obtained as a by-product of range data. Note that all of the pixels in the range image have corresponding reflectance values. In other words, the range image and the reflectance image are precisely and fundamentally aligned.

Using the reflectance image, we firstly propose a new smoothing technique using the trilateral filter by Choudury et al. [3] and reflectivity as a denoising technique of an image. In the proposed method, the trilateral filter is applied for not only the range image but also the corresponding reflectance image. By taking account of the properties of range and reflectance images, the proposed method can smooth range images while preserving geometric features such as jump and roof edges.

Next, we propose a new inpainting technique of a range image using a reflectance image and belief propagation. In this method, the deteriorated range values in a range image are recovered using not only the adjacent range values but also the continuity of the reflectance image.

In Section 2, an overview of the previous approaches will be presented. In Sections 3 and 4, we will propose two new denoising techniques for range images using reflectance images, that is, range image smoothing by the trilateral filter and range image inpainting by belief propagation. In Section 5, simulations and experiments using a laser scanner will be reported for the purpose of verifying the performance of the proposed techniques.

II. RELATED RESEARCH

Smoothing techniques for range images are classified into two categories: pixel-based or point-based techniques [4], [5], [6], [7] and mesh-based techniques [8], [9], [10], [11]. Raw range data acquired by range sensors is composed of a group of 3D points called a point-cloud. Pixel or point-based methods denoise the range image or the point-cloud directly without taking the continuity of pixels into account explicitly. On the other hand, mesh-based methods are applied to structured meshes, such as triangular patches, by considering the continuity of the vertexes in the structured meshes.

For the case in which a high-resolution gray-scale image and a low resolution range image are simultaneously captured from a range sensor, Diebel et al. [5] proposed a technique for estimating high-resolution range images by considering the Markov Random Field in high- and low-resolution range images and adjusting smoothing parameters according to the gradient of the high-resolution gray-scale image. Crabb et al. [12] and Chan et al. [6] also proposed an up-sampling technique using the joint bilateral filter [13]. Bohme et al. [11] proposed the denoising technique for a range image using the shape-from-shading technique [14]. They introduced an energy function consisting of the difference of the observed intensity and its estimation based on the Lambertian reflectance model and the continuity of the range image and the intensity. Then, the energy function

S. Oishi is with Graduate School of Information Science and Electrical Engineering, Kyushu University, 744 Motooka, Nishi-ku, Fukuoka 819-0395, Japan oishi@irvs.is.kyushu-u.ac.jp

R. Kurazume, Y. Iwashita, and T. Hasegawa are with Graduate Faculty of Information Science and Electrical Engineering, Kyushu University, 744 Motooka, Nishi-ku, Fukuoka 819-0395, Japan

978-1-61284-455-8/11/$26.00 ©2011 IEEE

is minimized by the non-linear conjugate gradient method so that the noise in the range image is suppressed.

On the other hand, several techniques based on the bilateral filter [15], which was developed as an edge-preserving filter for gray-scale images, have been proposed [9], [10], [4], [16]. Fleishman et al. [10] proposed a 3D edge preserving filter by applying the bilateral filter for the distance from a point to its adjacent points projected on a tangential plane (tangential component) and the distance from the adjacent points to the tangential plane (normal component). Jones et al. [9] proposed a similar technique using triangular meshes instead of tangential planes. However, these smoothing techniques are applied after converting from the point-cloud to the meshes and it is difficult to obtain the normal vectors stably from meshes that contain a great deal of noise. Moreover, in some cases, the construction of structured meshes from a noisy point-cloud is not a simple and trivial problem.

Miropolsky [4] proposed the geometric bilateral filter, which uses the distances from the adjacent points and the difference of normal directions for each point in the point-cloud. However, a stable solution of normal vectors from a noisy point-cloud has not yet been found.

While these methods can be considered as a simple extension of the bilateral filter for a gray-scale image to a range image, the technique proposed herein uses a reflectance image that corresponds one-to-one to the range image for smoothing the range image. Note that although we assume that the range and reflectance images have the same resolution, the proposed method can be applied to images having various resolutions using the joint bilateral filter [13].

For the case in which there are several holes in range data due to the occlusion or specular or weak reflection, Kawai et al. [17] proposed a completion technique of the 3D surfaces. They define an energy function based on the similarity of shapes, and select the best match which minimizes the energy function to fill in the holes of 3D geometry. Becker et al. [18] proposed a completion method using an additional color image of the same scene from a different viewpoint. Xu et al. [19] also proposed the technique which estimates missing geometry by learning association of surface normals to image patches in calibrated images.

On the other hand, several inpainting techniques based on belief propagation have been proposed [20], [21]. Pedro et al. [20] proposed an image completion method which takes the continuity of pixels into account by applying belief propagation. Komodakis et al. [21] proposed an exemplar-based inpainting technique using belief propagation. They introduced the Priority-BP that extends standard belief propagation for priority-based message scheduling and dynamic label pruning.

III. Smoothing Range Image Using the Trilateral Filter

In this section, we propose a new technique for smoothing a range image using the trilateral filter [3] and a reflectance image.

As mentioned above, conventional smoothing techniques for range data are mainly applied for a range image directly. On the other hand, we focus on a reflectance image that is acquired as a by-product of the range image for most range sensors. By taking the properties of both the range and reflectance images into account, the proposed technique can suppress noise in a range image while preserving geometric features such as jump and roof edges.

In the following sections, we introduce the conventional bilateral filter and a reflectance image captured by range sensors. The trilateral filter using a reflectance image is then described in detail.

A. Reflectance image

Optical range sensors, such as a laser scanner, obtain range data by measuring the round-trip time of a laser pulse reflected by an object. Figure 2(a) shows an example of a range image acquired by a 3D laser scanner (Fig. 1 [1]). On the other hand, most optical range sensors can measure the strength of the reflected laser pulse (reflectivity). Figure 2(b) shows a reflectance image that depicts reflectance values as a gray-scale image. As mentioned above, a unique reflectance value is determined for each pixel in the range image. In other words, the range image and the reflectance image are precisely and fundamentally aligned.

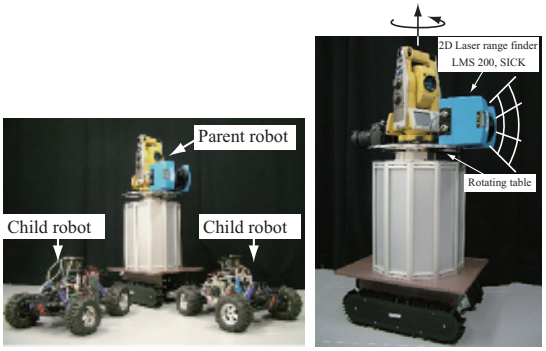

Fig. 1. Acquisition system of a panoramic range image [1]

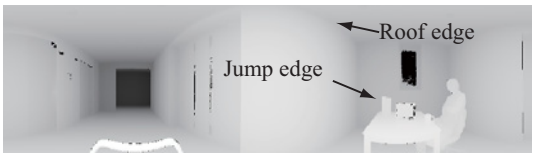

(a) Range image

(b) Reflectance image

Fig. 2. Range and reflectance images

B. Bilateral filter

The bilateral filter [15] is an edge-preserving smoothing filter that extends the Gaussian filter so that not only the

spatial relation but also the variation of the pixel intensity is considered. In the Gaussian filter, it is assumed that adjacent pixels may have similar intensities, and the weighted sum of neighbor pixels defined by a Gaussian distribution is calculated for each pixel as follows:

$$g_i = \frac{\sum_{j \in S_i} w_x(x_i, x_j) f_j}{\sum_{j \in S_i} w_x(x_i, x_j)} \tag{1}$$

$$w_x(x_i, x_j) = \frac{1}{\sqrt{2\pi}\sigma_x} e^{-\frac{|x_i - x_j|^2}{2{\sigma_x}^2}} \tag{2}$$

where x_i is the location of pixel i, g_i is a smoothed intensity value of pixel i, and f_j is the original intensity value of the pixel j, which is a neighbor S_i of pixel i. Here, $w_x(x_i, x_j)$ is the weight function determined by a Gaussian function with a variance of σ_x^2, and $|x_i - x_j|$ is the two-dimensional spatial distance between pixels i and j.

In addition to the Gaussian filter, the bilateral filter takes the variation of the intensity into consideration for image smoothing. More precisely, the bilateral filter determines the weight of the neighbor pixels according to not only the two-dimensional spatial relation but also the similarity of the intensity, as follows:

$$g_i = \frac{\sum_{j \in S_i} w_x(x_i, x_j) w_f(f_i, f_j) f_j}{\sum_{j \in S_i} w_x(x_i, x_j) w_f(f_i, f_j)} \tag{3}$$

$$w_f(f_i, f_j) = \frac{1}{\sqrt{2\pi}\sigma_f} e^{-\frac{|f_i - f_j|^2}{2{\sigma_f}^2}} \tag{4}$$

where $w_f(f_i, f_j)$ is the weight function for the intensity determined by a Gaussian function with a variance of σ_f^2 and $|f_i - f_j|$ is the difference in intensity of pixels i and j. Since the bilateral filter takes the difference in intensity into account, it is possible to preserve abrupt changes in intensity, such as roof and jump edges, which are blurred by Gaussian filters.

C. Extension of the bilateral filter to a range image

Let us apply the bilateral filter for a gray-scale image to a range image. In the same manner as Eqs. (2),(3) and (4), the bilateral filter for a range image can be defined as follows:

$$g_i = \frac{\sum_j w_x(x_i, x_j) w_f(f_i, f_j) f_i}{\sum_j w_x(x_i, x_j) w_f(f_i, f_j)} \tag{5}$$

$$w_x(x_i, x_j) = \frac{1}{\sqrt{2\pi}\sigma_x} e^{-\frac{|x_i - x_j|^2}{2{\sigma_x}^2}} \tag{6}$$

$$w_f(f_i, f_j) = \frac{1}{\sqrt{2\pi}\sigma_f} e^{-\frac{|f_i - f_j|^2}{2{\sigma_f}^2}} \tag{7}$$

where g_i and f_i are new and original range values at pixel i, and $w_x(x_i, x_j)$ and $w_f(f_i, f_j)$ are Gaussian functions for two-dimensional spatial and range information with variances of σ_x^2 and σ_f^2, respectively.

D. Trilateral filter with a reflectance image

The method mentioned above is a straightforward extension of the bilateral filter to a range image. However, as shown in Fig. 2(a), although abrupt changes of range values, such as a jump edge, are easily detected in a range image, moderate changes, such as a roof edge, are quite difficult to detect. Miropolsky [4] introduced the directional variation of normal vectors in order to emphasize these moderate changes in the range image. However, if we observe the reflectance image shown in Fig.2(b), it is easy to see that these moderate changes are clearly detected in the reflectance image.

Based on the above consideration, we propose a new filter that uses reflectance and range images simultaneously for smoothing a range image, as follows:

$$g_i = \frac{\sum_j w_x(x_i, x_j) w_f(f_i, f_j) w_d(d_i, d_j) f_i}{\sum_j w_x(x_i, x_j) w_f(f_i, f_j) w_d(d_i, d_j)} \tag{8}$$

$$w_x(x_i, x_j) = \frac{1}{\sqrt{2\pi}\sigma_x} e^{-\frac{|x_i - x_j|^2}{2{\sigma_x}^2}} \tag{9}$$

$$w_f(f_i, f_j) = \frac{1}{\sqrt{2\pi}\sigma_f} e^{-\frac{|f_i - f_j|^2}{2{\sigma_f}^2}} \tag{10}$$

$$w_d(d_i, d_j) = \frac{1}{\sqrt{2\pi}\sigma_d} e^{-\frac{|d_i - d_j|^2}{2{\sigma_d}^2}} \tag{11}$$

where f_i and d_i are the range and reflectance values in pixel i, and $w_x(x_i, x_j)$, $w_f(f_i, f_j)$, and $w_d(d_i, d_j)$ are Gaussian functions in the two-dimensional spatial, range, and reflectance domains with variances of σ_x^2, σ_f^2, and σ_d^2, respectively.

The filter given by Eq. (8) takes into account three kinds of information in range and reflectance images for smoothing a range image. In other words, it is an extension of the trilateral filter for images [3] so that it takes the variation of the reflectivity into consideration for range image smoothing. Thanks to a variety of properties in range and reflectance information, the proposed trilateral filter enables not only jump edges but also roof edges to be preserved in a range image, and the trilateral filter is expected to have higher performance for edge preservation than the simple expansion of the bilateral filter given by Eq. (5).

Consequently, the proposed smoothing technique for a range image is summarized as follows.

1) Acquire range and reflectance information by a time-of-flight range sensor.
2) Create range and reflectance images in which the values of each pixel in range and reflectance images are proportional to the range and reflectance values.
3) Apply the trilateral filter given by Eq. (8) using range and reflectance images and obtain a smoothed range image.
4) Construct a 3D model consisting of meshes from the smoothed range image.

IV. Range image inpainting by belief propagation

In the previous section, we proposed a range image smoothing technique using the trilateral filter and a reflectance image. Although this method is effective for range images that are corrupted by noise, a deteriorated range image that is missing part of the original image due to specular reflection or weak reflectivity of the laser pulse is difficult to repair. For recovering a range image that is missing part of the original image, this section proposes an image inpainting technique using belief propagation and a reflectance image.

A. Loopy belief propagation

Let us consider a graph P consisting of multiple nodes connected by multiple arcs. We assign label f_p to node p so that the following energy function is minimized.

$$E(f) = \sum_{p \in P} D_p(f_p) + \sum_{(p,q) \in N} W(f_p, f_q) \tag{12}$$

where $D_p(f_p)$ is a cost term for assigning label f_p to node p, and $W(f_p, f_q)$ is a penalty term if labels f_p and f_q are assigned to nodes p and q, respectively. Here, N indicates the neighbor nodes of node p.

In the framework of belief propagation, the following messages are repeatedly exchanged between the adjacent nodes in order to determine the optimum label f_p that minimizes the energy function:

$$m^t_{p \to q}(f_q) = \min_{f_p} \left(D_p(f_p) + W(f_p, f_q) + \sum_{s \in N(p) \setminus q} m^{t-1}_{s \to p}(f_p) \right) \tag{13}$$

After T iterations, optimum label f^*_q is determined so as to minimize the following cost function:

$$b_q(f_q) = D_q(f_q) + \sum_{p \in N(q)} m^T_{p \to q}(f_q) \tag{14}$$

B. Range image inpainting using a reflectance image

We apply belief propagation to a deteriorated range image and repair the image using a reflectance image. When we measure range data using a laser scanner, it often occurs that part of the range image is lost due to saturation of the reflectivity by specular reflection or a weak laser pulse reflected on a black surface. In most cases, not only the range information but also the reflectance information in this region is lost. The proposed inpainting technique for the range image consists of two steps. First, we repair the reflectance image by belief propagation in Section IV-A, because the reflectance image clearly contains roof and jump edges and the restoration of the reflectance image is easier than the restoration of the range image. Then, we apply belief propagation to the range image using the repaired reflectance image. In Section V, this two-step algorithm is demonstrated to be able to inpaint the range image more precisely than directly applying belief propagation to the range image.

Since belief propagation requires a huge memory and large calculation cost, the range image is first converted to a 256-level gray-scale image. Therefore, the number of labels to be assigned is 256, as expressed by integers from 0 to 255.

We define the cost term $D_p(f_p)$ for assigning label f_p to pixel p as

$$D_p(f_p) = 0 \tag{15}$$

for lost regions and

$$D_p(f_p) = \mid f_p - L_p \mid \tag{16}$$

for other regions, where L_p is the original label of pixel p. In addition, we consider the four-neighbor q of pixel p and define the cost function for assigning labels f_p and f_q as

$$W(f_p, f_q) = g(r_p, r_q)(f_p - f_q)^2 \tag{17}$$

where r_p and r_q are the intensity values of pixels p and q in the reflectance image, and $g(r_p, r_q)$ is a gain term that indicates the effect of the reflectance image.

$$g(r_p, r_q) = \alpha e^{-\beta(r_p - r_q)^2} \tag{18}$$

Equation (17) indicates that the neighboring pixel, which has a similar reflectance value is preferentially selected to repair a lost pixel in the deteriorated range image. In contrast, a pixel having a reflectance value that is changed discontinuously affects the repair of the range image only slightly.

V. Experiment

This section introduces the results of the preliminary experiments for image smoothing using the trilateral filter and image inpainting by belief propagation using simulated and actual range images. We conducted experiments with various parameters selected manually, and determined parameters used for the following experiments.

A. Range image smoothing by the trilateral filter

1) Simulation using a synthesized image: First, we performed the simulation experiments using the synthesized image shown in Fig. 3, which is a scene of a square box having sides of 1 meter in a room. A gray-scale image (Fig. 3(a)) is used instead of a reflectance image, and we added a random noise of 1 % of the range value to the range image.

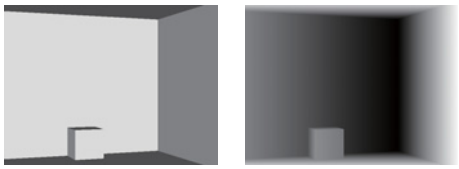

(a) Grayscale image (b) Range image

Fig. 3. Synthesized images used in the simulation experiment

Figure 4 shows the results obtained using the Gaussian filter, the bilateral filter, and the trilateral filter, respectively. Table I shows the RMS errors of the range images after applying these filters. In the experiment, the kernel size of each filter is 9×9 pixels, and the ranges of the range data and

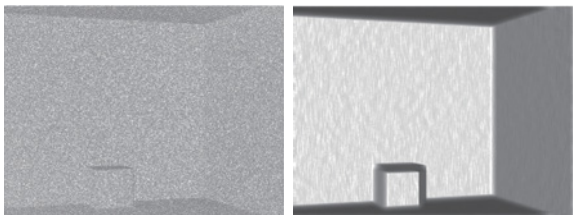

(a) 1% noise in depth values (b) Gaussian filter

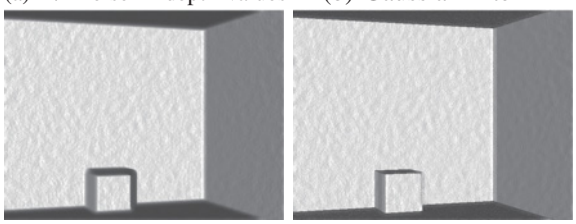

(c) Bilateral filter (d) Trilateral filter

Fig. 4. Denoised images by Gaussian filter, Bilateral filter and Trilateral filter

the reflectance data are 13,293 to 17,128[mm] and 0 to 255, respectively. The variances are set as $\sigma_x = 4.0$, $\sigma_f = 0.4$, and $\sigma_d = 6$.

As shown in Table I, the RMS error of the proposed trilateral filter is the smallest, and the proposed trilateral filter is verified to have high performance for range image smoothing and edge preservation.

TABLE I
RMS ERROR

	RMS [mm]
Original image	45.8
Gaussian filter	17.8
Bilateral filter	14.1
Trilateral filter (proposed)	11.7

2) Experiments with LIDAR: Next, we performed the experiments using the 3D laser measurement robot CPS-V shown in Fig. 1 [1]. The robot enables the surrounding range data to be captured by rotating the laser scanner (SICK, LMS200) by means of a rotary table. The image size is 200×721 pixels.

Figure 5 shows the two experimental conditions: a simple environment consisting mainly of roof edges (scene 1) and a more complex environment in which a human and other objects exist (scene 2) and a number of jump edges are observed. Figure 6 shows the range and reflectance images of these scenes captured by the measurement robot.

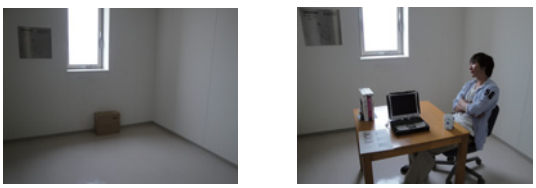

(a) Scene 1 (b) Scene 2

Fig. 5. Experimental setup

Range image Range image

Reflectance image Reflectance image

(a) Scene 1 (b) Scene 2

Fig. 6. Range and reflectance images

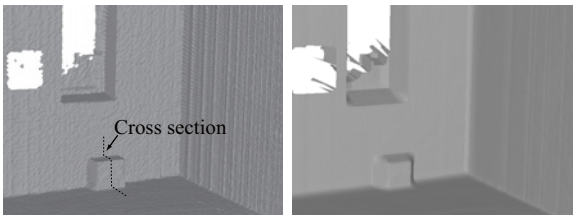

(a) Original range image (b) Gaussian filter

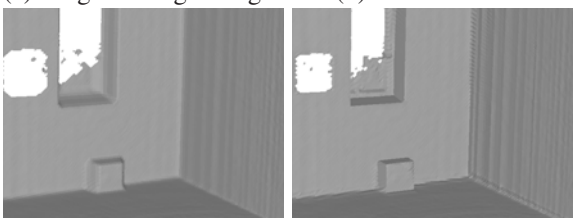

(c) Bilateral filter (d) Trilateral filter

Fig. 7. Experimental results for a simple environment

Figure 7 shows the results for scene 1 (Fig. 5(a)). In the experiment, we set the kernel size of the filters to be 9×9 pixels, and the ranges of the range data and the reflectance data are 275 to 8,191 [mm] and 0 to 255, respectively. The variances are $\sigma_x = 0.8$, $\sigma_f = 0.1$, and $\sigma_d = 7$ for the normalized range image.

Figure 7(a) is a 3-D model constructed from the original range image before applying smoothing filters. Several unexpected bumps appear on the surfaces of the walls and objects due to the noise in the range image. Figures 7(b), 7(c), and 7(d) show the images smoothed by the Gaussian filter, the bilateral filter, and the trilateral filter, respectively. These figures show that the surfaces of the walls are smoothed by the Gaussian filter and the bilateral filter. However, the edges of the box and the window frame are blurred. On the other hand, the trilateral filter can smooth the surfaces of the walls while preserving the edges of the box and the window frame.

Next, the results for scene 2 (Fig. 5(b)) are shown in Fig. 9. Similar to the experimental results for the scene 1, the Gaussian filter and the bilateral filter smooth the surfaces of the walls. In particular, the bilateral filter preserves the

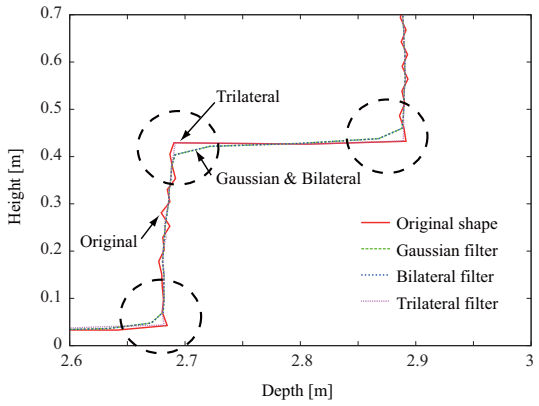

Fig. 8. Comparison of cross-section shape of the box

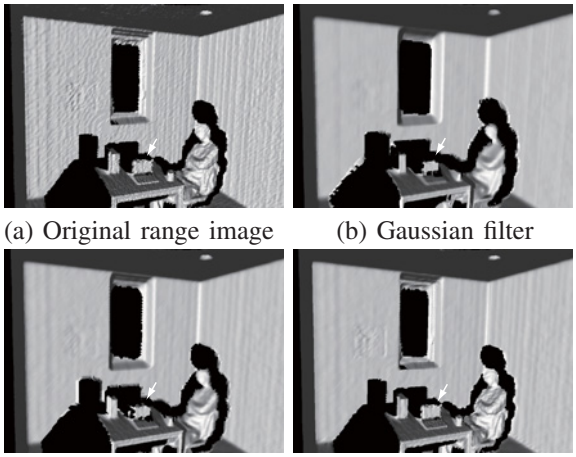

(a) Original range image (b) Gaussian filter

(c) Bilateral filter (d) Trilateral filter

Fig. 9. Experimental results for a complex environment

jump edges, such as the shape of the monitor, which is indicated by the arrow. However, the roof edges of walls, the face of the person, and the ruck of the clothes are blurred. On the other hand, the trilateral filter smoothes the range image successfully while preserving the jump and roof edges appropriately, as shown in Fig. 9(d).

B. Range image inpainting by belief propagation

We performed the simulation for range image inpainting by belief propagation, as described in Section IV. In the experiment, we prepared deteriorated reflectance and range images, which have a small missing region. The size of the image is 320×240 pixels, and the size of the missing part is 20×20 pixels. In this experiment, we use $\alpha = 0.75$ and $\beta = 1.0$.

Figures 11(a) and 11(b) show the original and deteriorated range images, and Figs. 11(c) and 11(d) show the deteriorated and repaired reflectance images. The inpainted range images after applying belief propagation 30 times are shown in Figs. 11(e) and 11(f). These images are repaired with and without the reflectance image, respectively. The RMS errors for these repaired images are compared in Table II.

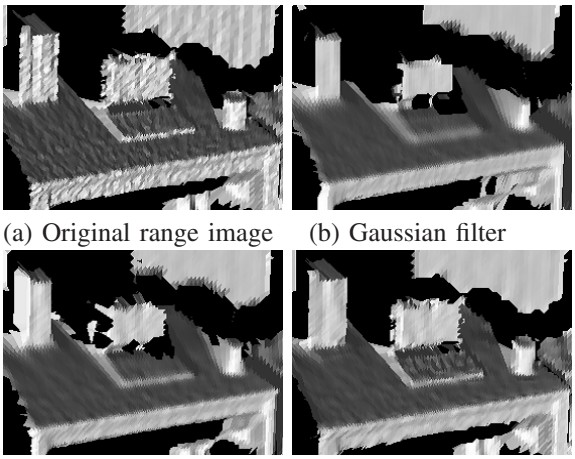

(a) Original range image (b) Gaussian filter

(c) Bilateral filter (d) Trilateral filter

Fig. 10. Partial enlarged views

Next, we performed the experiments using actual range and reflectance images taken by the laser scanner on the CPS-V robots (Fig.1). In this experiment, we use $\alpha = 0.75$ and $\beta = 0.5$. Figure 12 shows the 3-D models restored by two techniques, that is, the simple belief propagation for range images and the proposed two-step algorithm using reflectivity. Missing parts are recovered appropriately by both techniques and there is not big difference in terms of the image quality. To emphasise the difference of the two techniques, we prepared deteriorated range and reflectance images manually by cutting a part of a wall, and applied the simple belief propagation and the proposed technique. Figure 13 shows the restored wall after applying these techniques, and each RMS error is shown in Table III.

From these results, the range image inpainting is successfully carried out using the two-step algorithm with belief propagation and the reflectance image.

TABLE II

RMS ERROR FOR RANGE IMAGE INPAINTING

iteration	RMS[mm]	
	Without reflectance	With reflectance
12	36.24	29.01
30	28.99	10.68
50	29.44	10.64

TABLE III

RMS ERROR IN EXPERIMENTAL RESULTS FOR THE PERFORMANCE EVALUATION

	RMS [mm]
Without reflectance	7.68
With reflectance (2step)	1.44

VI. CONCLUSION

In the present paper, we proposed two denoising techniques of range images using reflectivity, namely, range

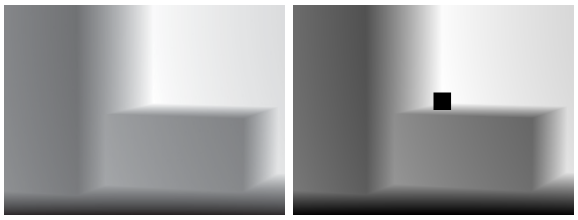

(a) Original range image (b)Deteriorated range image

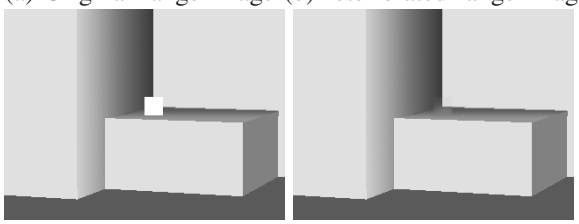

(c) Deteriorated reflectance image (d) Inpainted reflectance image

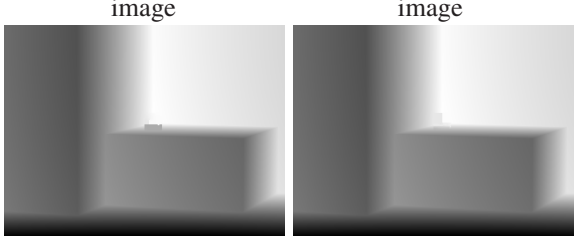

(e) Inpainted range image without reflectance image (f) Inpainted range image using reflectance image

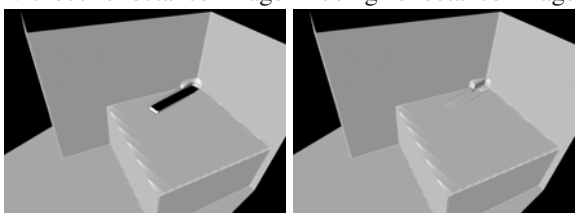

(g) Standard BP (h) Proposed method

Fig. 11. Range image inpainting by Belief Propagation

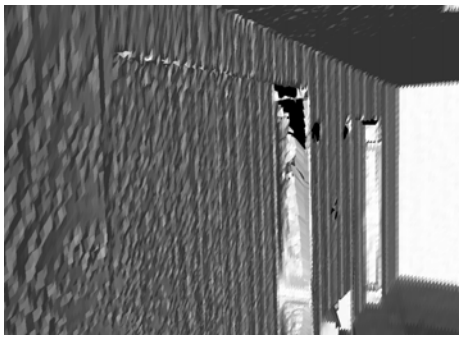

(a) Original 3D mesh model with a missing region

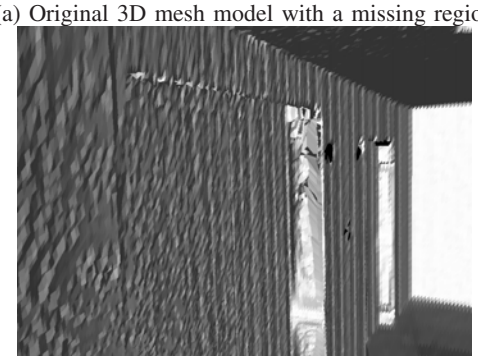

(b) The 3D mesh model after applying belief propagation

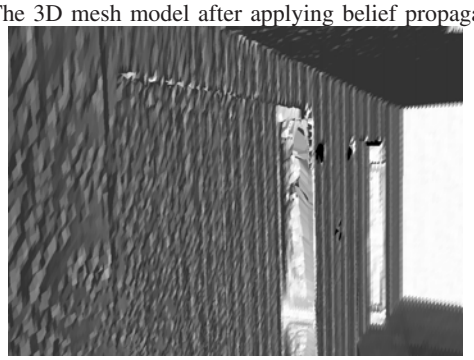

(c) The 3D mesh model after applying our two-step algorithm

Fig. 12. Experimental results for the range and reflectance images taken by the laser scanner

image smoothing by the trilateral filter and range image inpainting by belief propagation. By taking into account the properties of range and reflectance images, the proposed trilateral filter can suppress noises in range images while preserving geometric features such as jump and roof edges. Belief-propagation-based range image inpainting was also proposed to recover deteriorated range images using not only the adjacent range values but also the continuity of the reflectance image. We conducted experiments using a synthesized image and actual range images and verified that the proposed denoising techniques successfully suppress noises and repair deteriorated range images.

Since the reflectance image is obtained as a by-product of range data, the proposed method has several advantages. For example, no additional measurements or instruments are required, and, unlike conventional camera images, the reflectance image is not affected by lighting conditions.

In the future, we will discuss the optimum parameters for the proposed technique and perform quantitative evaluation for a variety of scenes.

REFERENCES

[1] R. Kurazume, Y. Noda, Y. Tobata, K. Lingemann, Y. Iwashita, and T. Hasegawa, "Laser-based geometric modeling using cooperative multiple mobile robots," in *Proc. IEEE International Conference on Robotics and Automation*, 2009, pp. 3200–3205.

[2] R. Kurazume, K. Noshino, Z. Zhang, and K. Ikeuchi, "Simultaneous 2D images and 3D geometric model registration for texture mapping utilizing reflectance attribute," in *Proc. of Fifth Asian Conference on Computer Vision (ACCV)*, 2002, pp. 99–106.

[3] P. Choudhury and J. Tumblin, "The trilateral filter for high contrast images and meshes," in *Eurographics Symposium on Rendering*, 2003, pp. 1–11.

[4] A. Miropolsky and A. Fischer, "Reconstruction with 3D geometric bilateral filter," in *SM '04: Proceedings of the ninth ACM symposium on Solid modeling and applications*. Aire-la-Ville, Switzerland, Switzerland: Eurographics Association, 2004, pp. 225–229.

[5] J. Diebel and S. Thrun, "An application of Markov random fields to range sensing," in *Proceedings of Conference on Neural Information Processing Systems (NIPS)*. Cambridge, MA: MIT Press, 2005.

[6] D. Chan, H. Buisman, C. Theobalt, and S. Thrun, "A noise-aware filter for real-time depth upsamplingw," in *Workshop on Multi-camera and Multi-modal Sensor Fusion Algorithms and Applications*, 2008.

[7] M. Lindner, M. Lambers, and A. Kolb, "Sub-pixel data fusion and edge-enhanced distance refinement for 2D/3D images," *International*

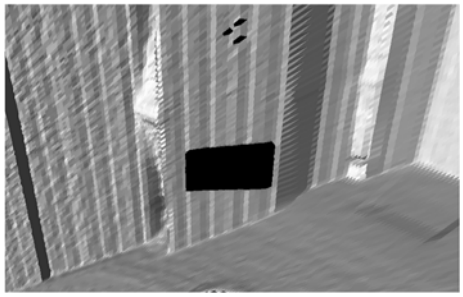

(a) Original 3D mesh model with a missing region

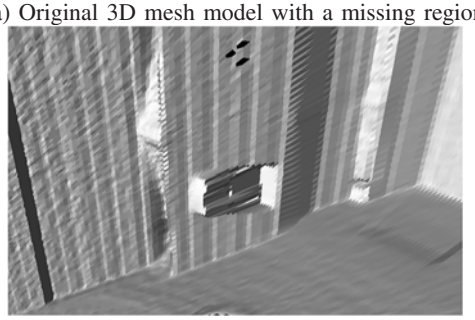

(b) The 3D mesh model after applying belief propagation

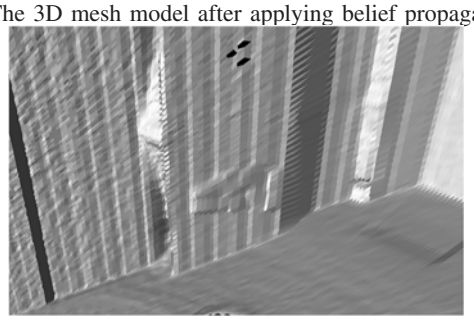

(c) The 3D mesh model after applying our two-step algorithm

Fig. 13. Experimental results for the performance evaluation

Journal on Intelligent Systems Technology and Application, vol. 5, no. 3/4, pp. 344–354, 2008.

[8] M. Desbrun, M. Meyer, P. Schro"der, and A. H. Barr, "Implicit fairing of irregular meshes using diffusion and curvature flow," in *SIGGRAPH '99*, 1999, pp. 317–324.

[9] T. R. Jones, F. Durand, and M. Desbrun, "Non-iterative, feature-preserving mesh smoothing," in *SIGGRAPH '03: ACM SIGGRAPH 2003 Papers*. New York, NY, USA: ACM, 2003, pp. 943–949.

[10] S. Fleishman, I. Drori, and D. Cohen-Or, "Bilateral mesh denoising," *ACM Transactions on Graphics*, vol. 22, no. 3, pp. 950–953, 2003.

[11] M. Bohme, M. Haker, T. Martinetz, and E. Barth, "Shading constraint improves accuracy of time-of-flight measurements," in *Computer Vision and Pattern Recognition Workshops, 2008. CVPRW '08. IEEE Computer Society Conference on*, 23-28 2008, pp. 1 –6.

[12] R. Crabb, C. Tracey, A. Puranik, and J. Davis, "Real-time foreground segmentation via range and color imaging," in *In Proc. of CVPR Workshop on Time-of-flight Computer Vision*, 2008, pp. 1–5.

[13] J. Kopf, M. Cohen, D. Lischinski, and M. Uyttendaele, "Joint bilateral upsampling," *ACM Transactions on Graphics (Proceedings of SIGGRAPH 2007)*, vol. 26, no. 3, p. 96, 2007.

[14] J.-D. Durou, M. Falcone, and M. Sagona, "Numerical methods for shape-from-shading: A new survey with benchmarks," *Comput. Vis. Image Underst.*, vol. 109, no. 1, pp. 22–43, 2008.

[15] C. Tomasi and R. Manduchi, "Bilateral filtering for gray and color images," in *ICCV '98: Proceedings of the Sixth International Conference on Computer Vision*. Washington, DC, USA: IEEE Computer Society, 1998, pp. 839–846.

[16] S. Yoshizawa, A. Belyaev, and H. peter Seidel, "Smoothing by example: Mesh denoising by averaging with similarity based weights," in *In Proceedings of the IEEE International Conference on Shape Modeling and Applications (2006)*. IEEE, 2006, pp. 38–44.

[17] N. Kawai, T. Sato, and N. Yokoya, "Surface completion by minimizing energy based on similarity of shape," in *Proc. IEEE Int. Conf. on Image Processing (ICIP2008)*, 2008, pp. 1532–1535.

[18] J. Becker, C. Stewart, and R. J.Radke, "Lidar inpainting from a single image," in *In Proceedings of the IEEE International Workshop on 3-D Digital Imaging and Modeling*, 2009.

[19] S.Xu, A.Georghiades, H.Rushmeier, J.Dorsey, and L.McMillan, "Image guided geometry inference," in *Proc. 3rd Int. Symp. on 3DPVT*, 2006, pp. 310–317.

[20] P. F. Felzenszwalb and D. P. Huttenlocher, "Efficient belief propagation for early vision," *International Journal of Computer Vision*, vol. 70, no. 1, 2006.

[21] N. Komodakis and G. Tziritas, "Image completion using global optimization," in *Proc. IEEE Conf. on Computer Vision and Pattern Recognition*, 2006, pp. 442–452.